White light-induced drift of particles with a hyperfine splitting of levels

S. N. Atutov, A. I. Parkhomenko, S. P. Pod'yachev, and A. M. Shalagin

Institute of Automation and Electrometry, Siberian Branch of the Academy of Sciences of the USSR, Novosibirsk

(Submitted 20 February 1990)
Zh. Eksp. Teor. Fiz. **99**, 378–392 (February 1991)

An investigation was made of the light-induced drift of single-component absorbing particles with a hyperfine splitting of the ground-state levels. This drift is induced by radiation with a constant spectral intensity (white light) incident on an optically dense medium. The drift is induced because as the light propagates a dip of a specific shape appears in the spectrum of light in the vicinity of an absorption line. In the absence of collisional transitions between the hyperfine components the drift velocity can reach $\sim 5\%$ of the maximum possible drift velocity when the spectrum of light is established artificially.

1. INTRODUCTION

The light-induced drift (LID) of gases[1,2] is one of the strongest effects of radiation on the translational motion of gas particles. The drift velocity induced by laser excitation may reach thermal values.[3] Experiments have shown[4,5] that the LID velocity of atoms can amount to several tens of meters per second and that atoms may collect and form a layer less than 1 mm thick.

The LID is important in tackling such scientific and practical tasks as preparation of chemically pure substances, isotope separation and enrichment, detection of microimpurities in large volumes of gases, determination of the diffusion coefficients of particles in excited states (see, for example, the experiments reported in Refs. 5–8).

Attention has recently been drawn to a possible manifestation of the LID in astrophysical objects.[9] In particular, the LID in stellar atmospheres was used in Ref. 9 to explain the phenomenon of chemically peculiar stars. The LID appears if the radiation is spectrally inhomogeneous in the vicinity of a Doppler absorption line and if this inhomogeneity is asymmetric relative to the center of the absorption line. Such conditions are established in a stellar atmosphere when it is crossed by thermal radiation from the interior of a star and it has an initially smooth spectrum (Fraunhofer absorption lines). The asymmetry of the emission spectrum relative to the center of a line representing a given element is due to a nearby Fraunhofer absorption line of a different element or a different isotope of the same element.

The quantitative solution for the simplest ("laboratory") variant of the LID due to white light was given in Ref. 10. It was assumed that a gas mixture consisting of two types of absorbing particles with adjacent absorption lines and of buffer particles is exposed to low-intensity radiation with a constant spectral intensity. The concentration of the particles at the entry to the mixture was assumed to be given. The case of a medium optically thin at right-angles to the beam was considered. Under these conditions the LID may result in a large increase of the concentration of one of the components of the absorbing particles and a large reduction in the concentration of the other component at the exit (relative to the incident radiation) end of the medium.[10] This quantitative result demonstrates that, in principle, it should be possible to account for the phenomenon of chemically peculiar stars by LID effects.

It was shown in Ref. 11 that drift induced by white light is, in principle, possible also when an absorbing gas consists of just one kind of particle with a hyperfine splitting of the ground state under conditions when the components of the hyperfine structure (HFS) are pumped optically. However, a detailed description of the effect was not given in Ref. 11. Our aim will be to analyze the behavior of this effect as a function of the spacing between the HFS components, of the ratio of the homogeneous and Doppler absorption line widths, of the intensity of the radiation, and of the sign of the difference between the transport frequencies of collisions in the ground and excited states, as well as to analyze the effect for large optical thicknesses of the absorbing medium and to obtain simple analytic expressions describing the LID in some limiting cases. This detailed investigation reveals a number of nontrivial aspects of the LID. We also consider the possibility of white-light-induced drift of particles with hyperfine splitting of the ground state in the absence of optical pumping of the HFS components.

2. LIGHT-INDUCED DRIFT IN A RADIATION FIELD WITH AN ARBITRARY SPECTRAL COMPOSITION

Consider the interaction between radiation with an arbitrary spectral composition and absorbing particles which are mixed with buffer particles. The energy level scheme of the absorbing particles is shown in Fig. 1. Here, the levels n and l are the components of the hyperfine structure of the ground state and g_i is a statistical weight of an ith level ($i = n, l, m$). The collisions between the absorbing particles will be neglected and it will be assumed that the buffer gas concentration is much higher than that of the absorbing gas.

Such a level scheme is suitable for the description of the LID of alkali metal atoms. In fact, the ground state of these atoms is split into two hyperfine components. The spacing between them is comparable to or greater than the Doppler width of the absorption lines and, therefore, the ground state can be modeled by two levels (n and l). The level m represents a group of levels which are the components of the HFS of the excited states $P_{1/2}$ or $P_{3/2}$. Such a representation of a group of levels by one is possible because in the case of alkali metal atoms the hyperfine splitting of these excited states is usually small compared with the Doppler absorption line width.

The interaction of the particles with radiation can be

 0038-5646/91/020210-09$03.00

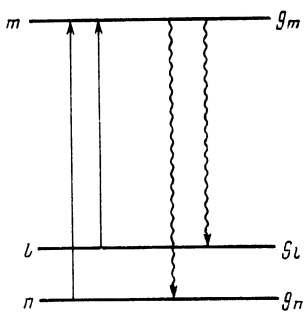

FIG. 1. Energy level scheme. The straight arrows represent transitions under the influence of external radiation and the wavy arrows represent spontaneous radiative transitions.

described by the following equations for the density matrix:[12]

$$\left(\frac{\partial}{\partial t}+\mathbf{v}\nabla+\Gamma_m\right)\rho_m(\mathbf{v})=S_m(\mathbf{v})+N[P_n(\mathbf{v})+P_l(\mathbf{v})],$$
$$\left(\frac{\partial}{\partial t}+\mathbf{v}\nabla\right)\rho_l(\mathbf{v})=S_l(\mathbf{v})+\Gamma_{ml}\rho_m(\mathbf{v})-NP_l(\mathbf{v}), \qquad (2.1)$$
$$\left(\frac{\partial}{\partial t}+\mathbf{v}\nabla\right)\rho_n(\mathbf{v})=S_n(\mathbf{v})+\Gamma_{mn}\rho_m(\mathbf{v})-NP_n(\mathbf{v}).$$

Here, $\Gamma_m=\Gamma_{mn}+\Gamma_{ml}$; Γ_{mn} and Γ_{ml} are the rates of $m\to n$ and $m\to l$ radiative transitions; N is the concentration of the absorbing particles; $S_i(\mathbf{v})$ are the collision integrals; and $P_n(\mathbf{v})$ and $P_l(\mathbf{v})$ are the probabilities of absorption of radiation per unit time as a result of m–n and m–l transitions in a particle traveling at a fixed velocity $\mathbf{v}$. We simplify the problem by considering only the weak field approximation and assuming that the rate of forced transitions is low compared with the radiative decay rate Γ_m of an excited level m and compared with the collision frequencies $\tilde{\nu}_i$ [see Eq. (2.7) below]:

$$P_n, P_l\ll\Gamma_m, \bar{\nu}_n, \bar{\nu}_l; \quad (P_i\equiv\langle P_i(\mathbf{v})\rangle). \qquad (2.2)$$

The angular brackets in the above equation and later denote integration with respect to the velocity $\mathbf{v}$.

The condition (2.2) means that the fraction of particles in an excited state is small and, moreover, that the populations of the HFS levels $\rho_n(\mathbf{v})$ and $\rho_l(\mathbf{v})$ have velocity distributions which are nearly Maxwellian. Moreover, we assume that the characteristic size l of a spatial inhomogeneity region and the characteristic time τ over which the parameters of the radiation and medium change satisfy the conditions $l\gg\bar{v}/\Gamma_i$ and $\tau\gg 1/\Gamma_i$ $(i=1, 2)$, where Γ_1 and Γ_2 are the homogeneous half-widths of the absorption lines due to the m–n and m–l transitions, respectively, and $\bar{v}$ is the most probable thermal velocity. Under these conditions the expression for $P_i(\mathbf{v})$ is

$$P_i(\mathbf{v})=\frac{N_i}{N}BY_i(\mathbf{v})W(\mathbf{v}),$$
$$B=\frac{\lambda^2}{4\hbar\omega}\frac{g_m}{g_n+g_l}\Gamma_m, \qquad Y_i(\mathbf{v})=\frac{1}{\pi}\int_{-\infty}^{\infty}\frac{\Gamma_j S(\omega')\,d\omega'}{\Gamma_j^2+(\omega'-\omega_{mi}-\mathbf{kv})^2},$$
$$N_i\equiv\langle\rho_i(\mathbf{v})\rangle, \quad (i=n, j=1;\ i=l, j=2). \qquad (2.3)$$

Here, $W(\mathbf{v})$ is the Maxwellian distribution of the velocities; B is the second Einstein coefficient; λ, ω, and $\mathbf{k}$ is the wavelength, frequency, and wave vector of the radiation; ω_{mi} is the frequency of the m–i transition; $S(\omega)$ is the spectral intensity of the radiation. In the expression for the Einstein coefficient B we took into account the circumstance that the ratio of the rates of radiative transitions from the level m to the HFS components n and l is governed by the ratio of their statistical weights:[13] $\Gamma_{ml}/\Gamma_{mn}=g_l/g_n$.

In our LID calculations we now go over from the rate equations (2.1) to the gasdynamic equations. We consider a one-dimensional problem where the radiation intensity is constant in a direction transverse to the z axis. We select the z axis along the direction of propagation of radiation. It follows from the equations of the system (2.1) multiplied by v_z and integrated with respect to the velocity $\mathbf{v}$ that

$$\frac{\partial}{\partial t}J+\frac{\partial P_z}{\partial z}=-(\nu_m j_m+\bar{\nu}_n j_n+\bar{\nu}_l j_l),$$
$$\left(\frac{\partial}{\partial t}+\Gamma_m+\nu_m\right)j_m+\frac{\partial P_{zm}}{\partial z}=N\langle v_z[P_n(\mathbf{v})+P_l(\mathbf{v})]\rangle, \qquad (2.4)$$
$$\left(\frac{\partial}{\partial t}+\nu_n\right)j_n+\frac{\partial P_{zn}}{\partial z}=\Gamma_{mn}j_m+\bar{\nu}_{nl}j_l-N\langle v_z P_n(\mathbf{v})\rangle,$$

where

$$J=j_m+j_n+j_l, \quad P_z=P_{zm}+P_{zn}+P_{zl},$$
$$j_i=\langle v_z\rho_i(\mathbf{v})\rangle, \quad P_{zi}=\langle v_z^2\rho_i(\mathbf{v})\rangle, \quad (i=n, l, m). \qquad (2.5)$$

The quantity MP_{zi} (M is the mass of an absorbing particle) represents the pressure exerted along the z axis by absorbing gas particles in the state i; j_i is the flux of the absorbing particles in the state i; J and MP_z are the total fluxes and the pressure of the absorbing particles. In the case under discussion when the incident radiation is weak, we have $MP_z=NT$, where T is the temperature of the gas in energy units. The system of equations (2.4) was derived above using the following relationships:

$$\langle v_z S_m(\mathbf{v})\rangle=-\nu_m j_m,$$
$$\langle v_z S_l(\mathbf{v})\rangle=-\nu_l j_l+\bar{\nu}_{ln}j_n, \qquad (2.6)$$
$$\langle v_z S_n(\mathbf{v})\rangle=-\nu_n j_n+\bar{\nu}_{nl}j_l.$$

Here, ν_m is the momentum-transfer frequency for elastic collisions between a particle in a level m and the buffer gas particles; $\bar{\nu}_{ji}$ is the rate of "transfer" of the flux j_i from the level i to the level j by collisions; ν_i $(i=n, l)$ is the rate of relaxation of the flux j_i at the level i due to elastic $(i\to i)$ and inelastic $(i\to j)$ scattering channels. The quantities

$$\tilde{\nu}_n=\nu_n-\bar{\nu}_{ln}, \quad \tilde{\nu}_l=\nu_l-\bar{\nu}_{nl} \qquad (2.7)$$

used in the system (2.4) are the frequencies representing elastic and inelastic collisions.

Before we tackle the solution of the system of equations (2.4), we note that the characteristic time of the "adjustment" of the fluxes j_i to the changes in the radiation parameters and medium is governed by the collision time ν_i^{-1}. We assume that the characteristic times for the parameters of the radiation and medium to change are longer than the microscopic times ν_i^{-1}. This allows us to ignore the time derivatives in the system (2.4). We also assume that

$$\frac{|\bar{\nu}_n-\bar{\nu}_l|}{\bar{\nu}_n}\ll 1. \tag{2.8}$$

Under these conditions we find that the system (2.4) yields the following equation for the total flux J of the absorbing particles:

$$J=Nu_{\text{LID}}-D\frac{dN}{dz},\quad D=\frac{\bar{v}^2}{2\bar{\nu}_n},\quad \bar{v}=\left(\frac{2T}{M}\right)^{1/2} \tag{2.9}$$

where D is the diffusion coefficient of the absorbing particles. The quantity u_{LID} in Eq. (2.9) is the LID velocity of the absorbing particles

$$u_{\text{LID}}=\tau_\sigma{}^n\langle v_z P_n(\mathbf{v})\rangle+\tau_\sigma{}^l\langle v_z P_l(\mathbf{v})\rangle$$
$$=\frac{\bar{v}}{\pi^{1/2}}B\int_{-\infty}^{\infty}dx\,S(x)\left[\tau_\sigma{}^n\frac{N_n}{N}\varphi_n(x-x_n)+\tau_\sigma{}^l\frac{N_l}{N}\varphi_l(x-x_l)\right], \tag{2.10}$$

where

$$S(x)=S(xk\bar{v})=S(\omega),$$
$$\tau_\sigma{}^n=\frac{1}{\Gamma_m+\nu_m}\left[\frac{\bar{\nu}_n-\nu_m}{\bar{\nu}_n}+\frac{\bar{\nu}_l-\bar{\nu}_n}{\bar{\nu}_n}\frac{(\nu_m\bar{\nu}_{ln}-\bar{\nu}_n\Gamma_{ml})}{q}\right],$$
$$\tau_\sigma{}^l=\tau_\sigma{}^n+\frac{\bar{\nu}_l-\bar{\nu}_n}{q},\quad q=\nu_n\nu_l-\bar{\nu}_{nl}\bar{\nu}_{ln}. \tag{2.11}$$

The expression for τ_σ^l is also obtained from the expression for τ_σ^n by transposing the indices $n\rightleftarrows l$. Equation (2.10) contains $\varphi_i(x-x_i)$, which is an odd function of $x-x_i$:

$$\varphi_i(x-x_i)=\text{Re}[z_i w(z_i)],$$
$$w(z_i)=\left[1+\frac{2i}{\pi^{1/2}}\int_0^{z_i}\exp t^2\,dt\right]\exp(-z_i^2),$$
$$z_i=(x-x_i)+iy_i,\quad x_i=\omega_{mi}/k\bar{v},\quad (i=n,l), \tag{2.12}$$
$$x=\omega/k\bar{v},\quad y_n=\Gamma_1/k\bar{v},\quad y_l=\Gamma_2/k\bar{v}.$$

In a bounded medium under steady-state conditions there is no absorbing particle flux ($J=0$) and the spatial variation in the particle concentration is described by

$$\frac{dN}{dz}=\frac{Nu_{\text{LID}}}{D}. \tag{2.13}$$

The drift velocity of Eq. (2.10) is expressed in terms of local values of the spectral intensity and of the fraction of particles in the levels n and l. These characteristics depend on the coordinate z and we have to find this dependence. We assume that the gaseous medium of interest is optically thin at right-angles to the z axis. Then, in the case of propagation along the z axis the spectral intensity of the radiation varies in accordance with the law

$$S(x)=S_0(x)\exp\left\{-\int_0^z dz[N_n\sigma_n(x-x_n)+N_l\sigma_l(x-x_l)]\right\},$$
$$\sigma_i(x-x_i)=\frac{\hbar\omega B}{\pi^{1/2}k\bar{v}}f_i(x-x_i), \tag{2.14}$$
$$f_i(x-x_i)=\text{Re}[w(z_i)],\quad (i=n,l),$$

where $S_0(x)$ is the spectral intensity of the radiation input to the medium ($z=0$); $\sigma_i(x-x_i)$ is the cross section representing the absorption of the radiation due to the m–i transition at a frequency $\omega=xk\bar{v}$; $f_i(x-x_i)$ is an even function of the argument $x-x_i$.

We shall find the velocity-integrated populations of the HFS levels N_n and N_l. We first consider the case of active collisional exchange between the levels n and l ($\nu_{ij}\sim\nu_i$). In the case of alkali metal atoms such a situation occurs, for example, when they collide with buffer particles that have a partly filled electron shell.[14] It follows from simple physical considerations that the populations N_n and N_l are close to equilibrium if in addition to the condition (2.2) the rates of the forced transitions are low compared with the frequencies of collisional exchange between the levels n and l:

$$P_n,\ P_l\ll\nu_{nl},\ \nu_{ln}. \tag{2.15}$$

We then have

$$\frac{N_i}{N}=w_i,\quad w_i=\frac{g_i}{g_n+g_l},\quad (i=n,l). \tag{2.16}$$

We now find the populations N_n and N_l in the absence of collisional exchange between the hyperfine components ($\nu_{nl}=\nu_{ln}=0$). In the case of alkali metal atoms this situation appears in an atmosphere of inert gases, because the cross sections of the collisional transitions $n\rightleftarrows l$ are then many orders of magnitude less than the gaskinetic cross sections.[15] We integrate, with respect to the velocity $\bar{v}$, the last three equations in the system (2.1) and assume that in the case of elastic collisions we have $\langle S_i(\mathbf{v})\rangle=0$ ($i=n,l,m$). We then obtain

$$\frac{\partial N_l}{\partial t}+\frac{\partial j_l}{\partial z}=\Gamma_{ml}N_m-NP_l,$$
$$\frac{\partial N_n}{\partial t}+\frac{\partial j_n}{\partial z}=\Gamma_{mn}N_m-NP_n. \tag{2.17}$$

The terms with the spatial derivative in the system (2.17) can be ignored if $u_{\text{LID}}\ll\bar{v}$, which is always satisfied in the case of a low radiation intensity (under consideration here) and then, under steady-state conditions, it follows from Eq. (2.17) that

$$\frac{P_n}{P_l}=\frac{\Gamma_{mn}}{\Gamma_{ml}}. \tag{2.18}$$

This important relationship shows that the ratio of the total probabilities of absorption of radiation as a result of the m–n and m–l transitions is independent of the radiation intensity and frequency. This relationship represents the process of optical pumping of the ground-state levels and is a consequence of the absence of collisional exchange between the hyperfine components n and l.

Applying the normalization condition $N_n+N_l\approx N$ [under the conditions of Eq. (2.2), we have $N_m\ll N$], we find from Eqs. (2.3) and (2.18) that

$$\frac{N_n}{N}=\frac{\Gamma_{mn}Y_l}{\Gamma_{mn}Y_l+\Gamma_{ml}Y_n},\quad \frac{N_l}{N}=1-\frac{N_n}{N},$$
$$Y_i=\langle Y_i(\mathbf{v})W(\mathbf{v})\rangle=\frac{1}{\pi^{1/2}}\int_{-\infty}^{\infty}f_i(x-x_i)S(x)\,dx,\quad (i=n,l). \tag{2.19}$$

We assume that, for example, narrow-band radiation is in resonance with the m–n transition and not with the m–l transition, so that $Y_l\ll Y_n$. It then follows from Eq. (2.19) that

$N_n \ll N_l \approx N$, i.e., almost all the particles are transferred to the level l, as expected in this case.

The relationships given by Eqs. (2.10), (2.13), (2.14), and (2.16) [or Eq. (2.19)] represent a closed system of equations which can be used to find the drift velocity at each point and to determine the spatial distribution of the particle concentration. We shall consider later the solutions of these equations under specific conditions.

3. WHITE-LIGHT-INDUCED DRIFT

We now discuss a situation in which a medium with an absorbing gas is illuminated with white light, i.e., when the radiation incident on the medium is characterized by a constant spectral intensity: $S_0(x) = S_0 = \text{const}$. Then, Eq. (2.10) for the drift velocity can be transformed conveniently by means of the relationship[16]

$$\frac{df_i(x-x_i)}{dx} = -2\varphi_i(x-x_i) \tag{3.1}$$

to the following form (later we shall give the explicit dependence of the various quantities on the dimensionless coordinate ξ):

$$\mathbf{u}_{\text{LID}}(\xi) = \frac{\mathbf{k}}{k}\frac{\bar{v}}{\pi^{1/2}} BS_0 \left[\tau_\sigma^n R_n(\xi) - \tau_\sigma^l R_l(\xi)\frac{d_n(\xi)}{d_l(\xi)}\right] \times \int_{-\infty}^{\infty} \varphi_n(x-x_n) I(x,\xi)\,dx, \tag{3.2}$$

where

$$I(x,\xi) = \frac{S(x,\xi)}{S_0} = \exp\{-[f_n(x-x_n)d_n(\xi) + f_l(x-x_l)d_l(\xi)]\},$$
$$d_i(\xi) = \int_0^{\xi} n(\xi)R_i(\xi)\,d\xi = \sigma\int_0^{\xi l_a} N_i(z)\,dz, \qquad R_i(\xi) = \frac{N_i(\xi)}{N(\xi)},$$
$$n(\xi) = \frac{N(\xi)}{N_0}, \qquad \xi = \frac{z}{l_a}, \qquad l_a = \frac{1}{\sigma N_0}, \qquad N_0 \equiv N(0), \tag{3.3}$$
$$\sigma = \frac{\lambda^2}{4\pi^{3/2}}\frac{\Gamma_m}{k\bar{v}}\frac{g_m}{g_n+g_l}, \qquad (i = n, l).$$

Here, $n(\xi)$ is the dimensionless concentration of the absorbing particles. The quantity $I(x, \xi)$ represents the profile of the radiation spectrum. At the entry to the medium the white light is characterized by $I(x, 0) = 1$. The parameter σ is the absorption cross section of monochromatic radiation at the center of a Doppler-broadened line when the spacing between the HFS components is zero. The quantity $d_i(\xi)$ represents the optical thickness of the medium when the radiation is absorbed as a result of the m–i transition. The sum

$$d_n(\xi) + d_l(\xi) \equiv d(\xi) = \int_0^{\xi} n(\xi)\,d\xi = \sigma\int_0^{\xi l_a} N(z)\,dz \tag{3.4}$$

is the total optical thickness of the medium.

In the absence of optical pumping of the HFS levels the fraction of the particles at these levels is $R_i(\xi) = w_i = \text{const}$ [see Eq. (2.16)]. In the opposite case (i.e., in the absence of collisional exchange between the HFS levels), it follows from Eq. (2.19) that

$$R_n(\xi) = \frac{w_n\int_{-\infty}^{\infty} f_l(x-x_l)I(x,\xi)\,dx}{\int_{-\infty}^{\infty}[w_n f_l(x-x_l) + w_l f_n(x-x_n)]I(x,\xi)\,dx}, \qquad R_l(\xi) = 1 - R_n(\xi). \tag{3.5}$$

Now consider Eq. (3.2). The integral in Eq. (3.2) resembles the integral of the velocity of drift of two-component absorbing particles under the influence of white light.[10] At the entry to the medium in the case of white light we have $I(x, 0) = 1$ and the drift velocity deduced from Eq. (3.2) is $\mathbf{u}_{\text{LID}}(0) = 0$ because the integrand $\varphi_n(x - x_n)$ is an odd function. The radiation becomes spectrally inhomogeneous in the course of propagation. The integral in Eq. (3.2) then vanishes only if $I(x, \xi)$, regarded as a function of x, is symmetric relative to the point $x = x_n$, which is possible only if the spacing between the HFS components is zero ($x_n = x_l$).

We now consider the factor in square brackets in front of the integral in Eq. (3.2). In the absence of optical pumping we have $R_i(\xi) = w_i$, so that this factor is $w_n(\tilde{\nu}_n - \tilde{\nu}_l)/q$. Consequently, if there is no optical pumping, the white-light-induced drift appears only when the transport collision frequencies at the HFS levels are different, i.e., if $\tilde{\nu}_n \neq \tilde{\nu}_l$ (which is equivalent to the condition $\tau_\sigma^n \neq \tau_\sigma^l$).

Under optical pumping conditions the LID appears when any pair of the frequencies $\tilde{\nu}_n$, $\tilde{\nu}_l$, and ν_m is different. This is due to the fact that the relative population of the HFS levels then varies along the coordinate ξ [$R_n(\xi)/R_l(\xi) \neq \text{const}$] and the factor in front of the integral in Eq. (3.2) vanishes for all values of ξ only if $\tau_\sigma^n = \tau_\sigma^l = 0$. Optical pumping appears in the course of propagation of white light through our medium because of the difference between the strengths of the lines representing the m–n and m–l transitions. On entering the medium, before spectral inhomogeneity sets in, the spectral intensity of the radiation in the vicinity of both lines is the same and there is no optical pumping [see Eq. (2.19)]. As the radiation propagates, a deeper dip appears near the stronger line (for example, that due to the m–l transition—see Fig. 3 below) than in the vicinity of the weaker line. Consequently, the spectral intensity of the radiation in the vicinity of the weak line is higher, which results in the transfer from the level n to the level l. This transfer enhances the asymmetry of the deformation of the radiation spectrum. The optical pumping effect reaches its maximum at some value of the optical thickness $d(\xi)$ and then falls to zero as $d(\xi)$ increases, so that if $d(\xi)$ is large, the depleted spectral interval broadens so much that the absorption occurs in the wings of the spectral lines and then the optical pumping effect does not occur. This is readily demonstrated on the basis of Eq. (2.19).

4. WHITE-LIGHT-INDUCED DRIFT IN THE ABSENCE OF OPTICAL PUMPING

We now consider in greater detail the LID in the absence of optical pumping of the HFS levels, i.e., subject to the condition (2.15). In this case we have $R_i(\xi) = w_i$ [see Eq. (2.16)], so that Eqs. (3.2) and (3.3) yield the drift velocity

$$\mathbf{u}_{\text{LID}}(\xi)=\frac{\mathbf{k}}{k}u_0 u(\xi), \tag{4.1}$$

where the parameter with the dimensions of the velocity is

$$u_0=\bar{v}\frac{Bw_nS_0(\tilde{\nu}_n-\tilde{\nu}_l)}{\pi^{1/2}q} \tag{4.2}$$

and the dimensionless velocity is described by

$$u(\xi)=\int_{-\infty}^{\infty}\varphi_n(x-x_n)I(x,\xi)dx,$$
$$I(x,\xi)=\exp\{-d(\xi)[w_nf_n(x-x_n)+w_lf_l(x-x_l)]\}. \tag{4.3}$$

For simplicity, we assume that the homogeneous half-widths of the absorption lines Γ_1 and Γ_2 due to the m–n and m–l transitions are equal ($\gamma_n=\gamma_l\equiv\gamma$). The drift velocity can be described by simple analytic expressions in the limiting cases of the homogeneous and Doppler broadening when the optical thickness is small. In the homogeneous broadening case, we have

$$u(\xi)=2w_ld(\xi)\frac{y\delta}{(\delta^2+4y^2)^2}, \tag{4.4}$$
$$\delta=x_n-x_l,\quad (y\gg 1,\quad d(\xi)\ll\pi^{1/2}y),$$

where δ is the spacing between the HFS components expressed in units of $k\bar{v}$. In the Doppler broadening case, we have

$$u(\xi)=\frac{\pi^{1/2}}{2^{1/2}}w_ld(\xi)\delta\exp(-\delta^2/2),\quad (y\ll 1,\ d(\xi)\ll 1). \tag{4.5}$$

It follows from Eqs. (4.4) and (4.5) that during the initial stage the drift velocity increases linearly as a function of the optical thickness $d(\xi)$.

Figure 2 shows a numerically calculated dependence of the drift velocity on the optical thickness. We can see that if $\delta=2$, $y=10^{-2}$, and $w_n=3/8$, the maximum of the drift velocity is reached when $d(\xi)\approx 4.5$ and amounts to $|u(\xi)|_{\max}\approx 0.15$. We now estimate the absolute velocity maximum $|\mathbf{u}_{\text{LID}}(\xi)|_{\max}$ in the specific case of sodium atoms. These atoms are characterized by $\Gamma_m=0.61\times 10^8\ \text{s}^{-1}$ and $B=1.6\cdot 10^{17}g_m/(g_n+g_l)\ \text{cm}^2\cdot\text{W}^{-1}\cdot\text{s}^{-2}$; the statistical weight of an excited state should be $g_m=24$ [which corresponds to $g_m/(g_n+g_l)=3$], because the white-light absorption occurs at the D_1 and D_2 lines. Under typical laboratory conditions the velocity of sodium atoms is $\bar{v}\sim 5\times 10^4$ cm/s and we have $\delta\approx 2$, and the value of $y=10^{-2}$ then corresponds to a collision frequency $\nu_i\sim 3\times 10^6\ \text{s}^{-1}$ ($i=n, l, m$). We assume that the spectral intensity of the radiation input to the medium is $S_0=2\times 10^{-3}\ \text{W}\cdot\text{cm}^{-2}\cdot\text{GHz}^{-1}$. Then, the probability of absorption input to the medium is $P_n+P_l=BS_0=1.5\cdot 10^5\ \text{s}^{-1}$, so that the conditions of Eqs. (2.2) and (2.15) are satisfied (in the case of active collisional exchange between the HFS components we have $\nu_{nl}\sim\nu_{ln}\sim\nu_i$—see Ref. 14). Consequently, if $|\tilde{\nu}_n-\tilde{\nu}_l|/\tilde{\nu}_n\sim 10^{-2}$, the maximum absolute drift velocity is $|\mathbf{u}_{\text{LID}}(\xi)|_{\max}\sim 0.3$ cm/s.

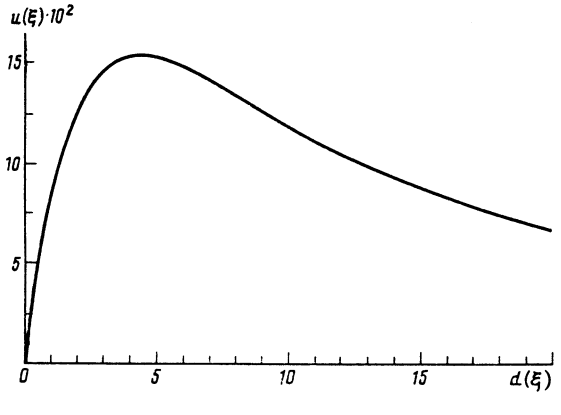

FIG. 2. Dependence of the drift velocity on the optical thickness $d(\xi)$ in the absence of optical pumping of the HFS levels. The calculations were carried out for $w_n=3/8$, $\delta=2$, and $y=10^{-2}$.

5. WHITE-LIGHT-INDUCED DRIFT IN THE PRESENCE OF OPTICAL PUMPING

In an analysis of the LID in the presence of optical pumping ($\nu_{nl}=\nu_{ln}=0$) we assume, for simplicity, that the homogeneous half-widths of the absorption lines due to the m–i transitions are equal ($\gamma_n=\gamma_l\equiv\gamma$) and the transport frequencies of collisions with the HFS levels are the same ($\nu_n=\nu_l$). The drift velocity of Eq. (3.2) can then be written conveniently in the form

$$\mathbf{u}_{\text{LID}}(\xi)=\frac{\mathbf{k}}{k}u_0u(\xi),\quad u_0=\bar{v}\frac{\nu_n-\nu_m}{\nu_n}\frac{BS_0}{\pi^{1/2}(\Gamma_m+\nu_m)}, \tag{5.1}$$

where we introduce the dimensionless velocity

$$u(\xi)=\left[R_n(\xi)-R_l(\xi)\frac{d_n(\xi)}{d_l(\xi)}\right]\int_{-\infty}^{\infty}\varphi(x-x_n)I(x,\xi)dx,$$
$$I(x,\xi)=\exp\{-[d_n(\xi)f(x-x_n)+d_l(\xi)f(x-x_l)]\}. \tag{5.2}$$

The relative fractions $R_i(\xi)$ of the particles in the HFS levels are given by Eq. (3.5). Since we are assuming that $\gamma_n=\gamma_l$, it follows that for identical values of the arguments we have $\varphi_n=\varphi_l$ and $f_n=f_l$, and the indices of these functions can be omitted. The parameter u_0 in Eq. (5.1) is approximately equal to the maximum attainable drift velocity of atoms when the spacing between the HFS components is zero and the radiation spectrum has a specific profile. More rigorously, $u_0/2$ is the velocity of drift of two-level atoms when the absorption line is Doppler-broadened and the radiation has a spectrum in the form of a semiinfinite step that begins at the atomic transition frequency.

Equation (2.13) for the concentration of the absorbing particles can also be rewritten conveniently in the dimensionless form

$$\frac{dn(\xi)}{d\xi}=au(\xi)n(\xi), \tag{5.3}$$

where

$$a=\frac{l_a}{l_0}=\frac{\nu_n-\nu_m}{\Gamma_m+\nu_m}\frac{2S_0}{\hbar cN_0},\quad l_0=\frac{D}{u_0}. \tag{5.4}$$

The system of equations (5.1)–(5.3) with the boundary condition $n(0)=1$ is closed and it describes the changes in the spectral intensity of the radiation, in the drift velocity, and in the concentration of the absorbing particles.

The drift velocity and the fractions of the particles at

the HFS levels can be described by simple analytic expressions in the limiting cases of the Doppler or homogeneous broadening provided the optical thickness is small. This can be done by expanding the exponential function in Eq. (5.2) in a series and noting that near input to the medium we have $n(\xi)\approx 1$ and $d(\xi)\approx\xi$. In the Doppler-broadening case, we obtain

$$R_n(\xi)=w_n\left\{1-\frac{d(\xi)}{2^{1/2}}w_l(w_l-w_n)[1-\exp(-\delta^2/2)]\right\},$$

$$u(\xi)=-d^2(\xi)\frac{\pi^{1/2}}{8}w_nw_l(w_l-w_n)\delta[\exp(-\delta^2/2)-\exp(-\delta^2)],$$

$$\delta=x_n-x_l,\quad (y\ll 1,\quad d(\xi)\approx\xi\ll 1). \qquad (5.5)$$

In the homogeneous-broadening case, we have similarly

$$R_n(\xi)=w_n\left[1-\frac{d(\xi)}{2\pi^{1/2}y}w_l(w_l-w_n)\frac{\delta^2}{\delta^2+4y^2}\right],$$

$$u(\xi)=-\frac{d^2(\xi)}{2\pi^{1/2}}w_nw_l(w_l-w_n)\frac{\delta^3}{(\delta^2+4y^2)^3}, \qquad (5.6)$$

$$(y\gg 1,\quad d(\xi)\approx\xi\ll\pi^{1/2}y).$$

It follows from the systems of equations (5.5) and (5.6) that the fraction of particles in an HFS level with the lowest statistical weight decreases as a function of the distance ξ from the entry to the medium [or the optical thickness $d(\xi)$]. During the initial stage the drift velocity rises quadratically with ξ. If the statistical weights are equal ($w_n = w_l$), there is no LID and no optical pumping.

Equations (5.5) and (5.6) may be useful in forecasting the degree of manifestation of the LID: a steeper rise of $u(\xi)$ during the initial stage generally corresponds to a higher value of $u(\xi)$ at the maximum (see Figs. 5–7 below).

6. RESULTS OF NUMERICAL CALCULATIONS; DISCUSSION

Figures 3–10 give the results of numerical calculations carried out using Eqs. (5.1)–(5.3). Figure 3 demonstrates the evolution of the radiation spectrum as the optical thickness $d(\xi)$ increases. Figure 4 illustrates the effect of optical pumping on the HFS levels. As expected, optical pumping becomes stronger when the spacing δ between the HFS components increases. However, for $\delta\gtrsim 3$, the rise of δ hardly changes the maximum magnitude of the effect. We note that Eq. (5.5) predicts the same optical pumping behavior when

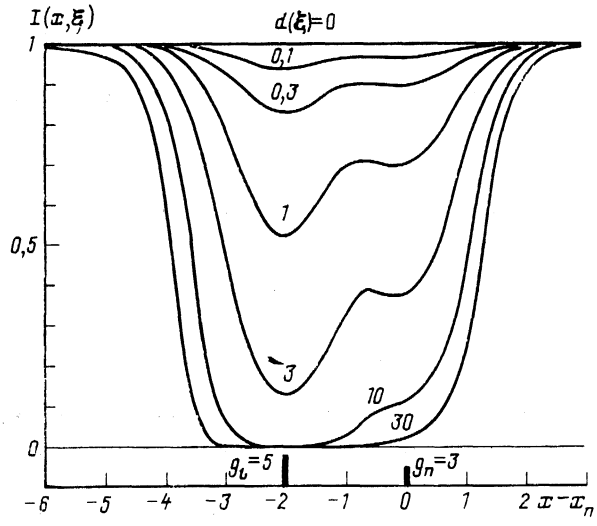

FIG. 3. Evolution of the radiation spectrum on increase in the optical thickness $d(\xi)$ under optical pumping conditions; the calculations were carried out for $w_n = 3/8$, $\delta = 2$, and $y = 10^{-2}$; the positions of the HFS levels are shown schematically on the abscissa.

the parameter δ is varied. The influence of the parameter y on the optical pumping is different: the smaller the parameter y the stronger the pumping (Fig. 4). The behavior of the populations of the HFS levels considered as a function of the optical thickness $d(\xi)$ was discussed above in connection with an analysis of Eq. (3.2) and it is confirmed by the plot of $R_n(\xi)$ in Fig. 4.

Figures 5–7 give the dependence of the drift velocity on the optical thickness $d(\xi)$ for different values of the parameters y and δ. The lower the value of y, the higher the maximum velocity and the wider the range of optical densities in which the drift velocity is significant compared with its maximum value (Fig. 5). For $y = 10^{-2}$, the maximum drift velocity is reached when the spacing between the HFS components is $\delta\approx 2$ (see Figs. 5 and 6); it should be noted that $\delta\approx 2$ is typical of sodium atoms under the usual experimental conditions when the temperature is $T\sim 300$–500 K. In the range of large optical thicknesses the drift velocity changes its sign and the amplitude of the maximum of this "reverse" velocity

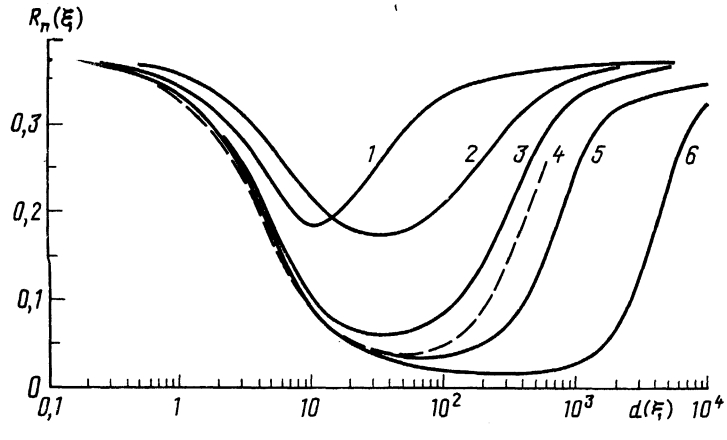

FIG. 4. Dependence of the fraction $R_n(\xi)$ of particles at an HFS level n on the optical thickness $d(\xi)$; the initial conditions are $R_n(0) = w_n = 3/8$: *1)* $\delta = 2$, $y = 10^{-1}$; *2)* $\delta = 1$, $y = 10^{-2}$; *3)* $\delta = 2$, $y = 10^{-2}$; *4)* $\delta = 3$, $y = 10^{-2}$; *5)* $\delta = 5$, $y = 10^{-2}$; *6)* $\delta = 2$, $y = 10^{-3}$.

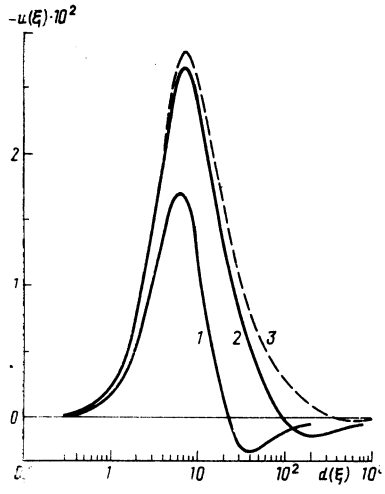

FIG. 5. Dependences of the drift velocity on the optical thickness $d(\xi)$; calculations are carried out for $w_n = 3/8$ and $\delta = 2$: 1) $y = 10^{-1}$; 2) $y = 10^{-2}$; 3) $y = 10^{-3}$.

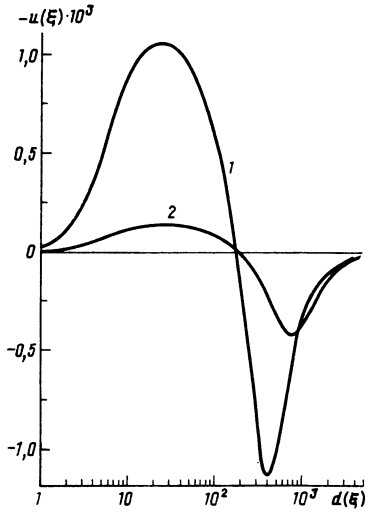

FIG. 7. Same as Fig. 6, but calculations for $w_n = 3/8$ and $y = 10^{-2}$: *1*) $\delta = 4$; *2*) $\delta = 5$.

increases with the parameter δ. For $y = 10^{-2}$, the maxima of the positive and negative drift velocities become comparable for $\delta \approx 4$, whereas in the range $\delta > 4$ the negative velocity becomes higher (Fig. 7). Analysis shows that this reversal of the sign of the velocity is due to reversal of the sign of the factor in front of the integral in Eq. (5.2).

If $y = 10^{-2}$ and $\delta = 2$, the maximum drift velocity occurs when the optical thickness is $d(\xi) = 7$ $[|u(\xi)|_{\max} = 2.65 \cdot 10^{-2}]$, whereas for $y = 0.1$ and $\delta = 2$ the maximum of $u(\xi)$ corresponds to $d(\xi) = 6.4$ $[|u(\xi)|_{\max} = 1.71 \cdot 10^{-2}$—see Fig. 5]. We estimate the maximum values of the absolute drift velocity from Eq. (5.1) using the Na–Ar system as an example. In the case of this mixture the relative difference between the transport collision frequencies of the sodium atoms is $(\nu_m - \nu_n)/\nu_n = 0.29$ (Ref. 17). The value of $\delta = 2$ for the sodium atoms means that the temperature of the mixture is $T = 376$ K. The parameter $y = 10^{-2}$ corresponds to the argon pressure $P_{Ar} = 0.5$ torr (at this pressure we can use the diffusion coefficient of sodium atoms to find $\nu_n = 3 \times 10^6$ s^{-1}), whereas the parameter $y = 0.1$ corresponds to $P_{Ar} = 10.4$ torr ($\nu_n = 6 \times 10^7$ s^{-1}). We assume that the spectral intensity of the radiation at the entry to the medium is $S_0 = 2 \times 10^{-3}$ W·cm^{-2}·GHz^{-1}. Consequently, the maximum drift velocity of sodium atoms in an argon atmosphere is $|\mathbf{u}_{LID}(\xi)|_{\max} = 0.5$ cm/s at an argon pressure $P_{Ar} = 0.5$ torr and $|\mathbf{u}_{LID}(\xi)|_{\max} = 0.2$ cm/s at $P_{Ar} = 10.4$ torr.

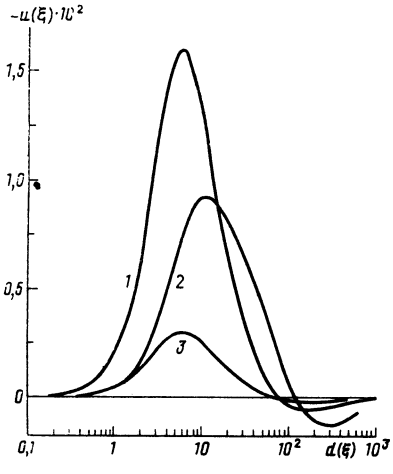

FIG. 6. Dependence of the drift velocity on the optical thickness $d(\xi)$ calculated for different spacings δ between the HFS components; calculations carried out for $w_n = 3/8$, $y = 10^{-2}$: *1*) $\delta = 1$; *2*) $\delta = 3$; *3*) $\delta = 0.5$.

Figures 8 and 9 show how the dimensionless particle concentration $n(\xi)$ depends on the dimensionless coordinate ξ in the case of negative values of the parameter a (i.e., when $\nu_n < \nu_m$). We now estimate numerically the parameter a for the Na–Ar mixture. We assume that the constant concentration of the absorbing particles $N_0 = 10^8$ cm^{-3} is maintained under experimental conditions at the entry to the medium. Then, if $S_0 = 2 \times 10^{-3}$ W·cm^{-2}·GHz^{-1}, it follows from Eq. (5.4) that we have $a = -270$ at an argon pressure $P_{Ar} = 10.4$ torr and $a = -30$ at $P_{Ar} = 0.5$ torr.

It is clear from Fig. 8 that for $a < 0$ and Doppler broadening ($y \ll 1$) the maximum change in the particle concentration corresponds to the spacing $\delta \approx 2$ between the HFS components. For $\delta = 3$, the change in $n(\xi)$ is greater than for $\delta = 1$, although the maximum drift velocity is less in the first case than in the second (a similar result also follows from a comparison of the cases when $\delta = 4$ and $\delta = 0.5$). This is because an increase in δ increases also the size of the region $\Delta\xi$ [or the optical thickness $\Delta d(\xi)$] in which the drift velocity does not show a reversal of the sign (Figs. 6 and 7). If the coordinate ξ is sufficiently large, the particle concentration falls and it may approach zero because of a change in the initial sign of the drift velocity.

It is clear from Fig. 9 that for given values of δ and a the concentration maximum $n(\xi)$ increases with reduction in the parameter y. However, if the maximum drift velocity changes by a factor of just 1.05 (Fig. 5) as we go over from $y = 10^{-2}$ to $y = 10^{-3}$ (for $\delta = 2$), we find that the particle concentration maximum increases by a factor of 2 (if $\delta = 2$, then $a = -100$). This is because the smaller the parameter

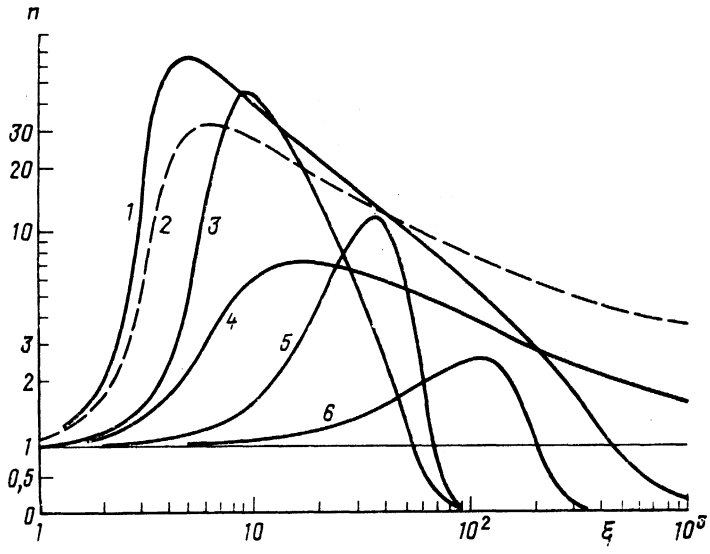

FIG. 8. Dependence of the particle concentration n on the coordinate ξ for different spacings δ between the HFS components; calculations carried out for $w_{\parallel} = 3/8$, $y = 10^{-2}$, and $a = -100$: *1*) $\delta = 2$; *2*) $\delta = 1$; *3*) $\delta = 3$; *4*) $\delta = 0.5$; *5*) $\delta = 4$; *6*) $\delta = 5$ [the scale is linear for $n(\xi) < 1$].

y, the greater the width of the region $\Delta d(\xi)$ characterized by a constant sign of the drift velocity.

It is also clear from Fig. 9 that for the same values of δ and y the maximum concentration is approximately proportional to the value of the parameter a. The parameter a in turn is inversely proportional to the particle concentration N_0 entering the medium and, consequently, the lower the value of N_0 the greater the change in the concentration. This dependence is due to the fact that at low values of N_0 the optical thickness $d(\xi)$ at which the drift velocity changes its sign is reached at higher values of z. In other words, if N_0 is low, then the size of the region where the effects of the LID accumulate is large.

Figure 10 illustrates the dependence of the particle concentration on the coordinate ξ in the case when $a > 0$ (provided $\nu_{\parallel} > \nu_{\perp\perp}$). If the value of the parameter a is sufficiently large, the particle concentration decreases right down to zero on increase in ξ. However, when the parameter a decreases, the behavior of $n(\xi)$ becomes qualitatively different: during the initial stage the concentration no longer falls to zero and then it rises by a large factor, reaching a constant value at high ξ. If the parameters δ and y are constant, the change in the nature of the behavior of $n(\xi)$ is threshold-like in respect of a. The dependence of the behavior of $n(\xi)$ on the parameter a is easily understood from the dependence of the drift velocity on the optical thickness (see, for example,

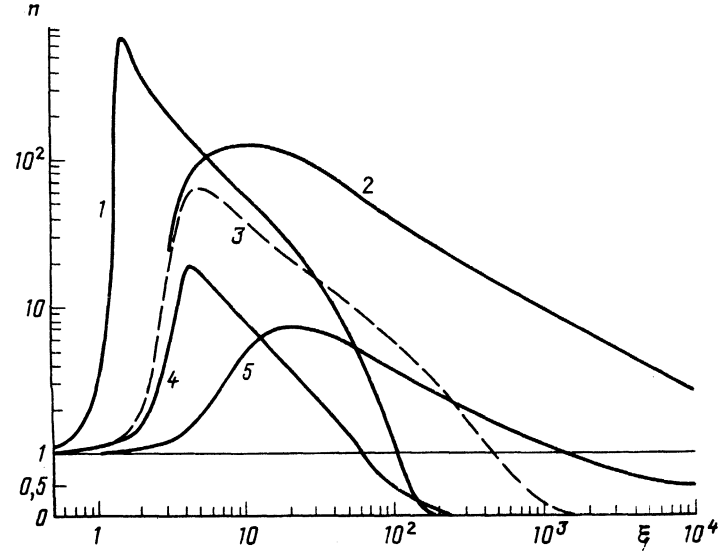

FIG. 9. Dependence of the particle concentration n on the coordinate ξ calculated for different values of the parameters y and a, assuming that $w_{\parallel} = 3/8$ and $\delta = 2$: *1*) $y = 10^{-2}$, $a = -10^3$; *2*) $y = 10^{-1}$, $a = -100$; *3*) $y = 10^{-2}$, $a = -100$; *4*) $y = 10^{-1}$, $a = -100$; *5*) $y = 10^{-2}$, $a = -10$ [the scale is linear for $n(\xi) < 1$].

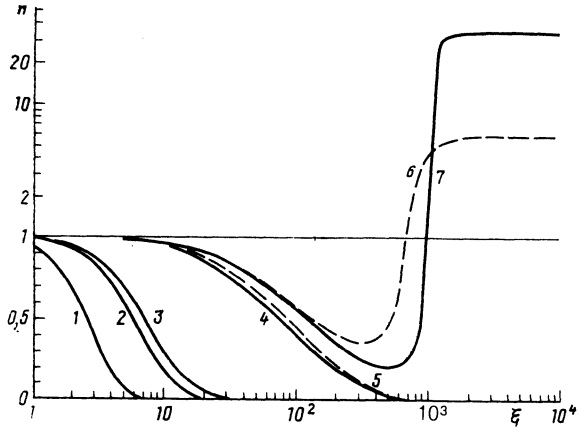

FIG. 10. Dependences of the particle concentration n on the coordinate ξ for positive values of the parameter a, calculations carried out assuming that $w_{\parallel} = 3/8$: 1) $\delta = 2, y = 10^{-1}, a = 100$; 2) $\delta = 2, y = 10^{-3}, a = 10$; 3) $\delta = 2, y = 10^{-1}, a = 10$; 4) $\delta = 4, y = 10^{-2}, a = 10$; 5) $\delta = 5, y = 10^{-2}, a = 70$; 6) $\delta = 4, y = 10^{-2}, a = 6$; 7) $\delta = 5, y = 10^{-2}, a = 50$ [the scale is linear for $n(\xi) < 1$].

Fig. 7). In fact, at high values of a the particle concentration falls rapidly to zero at a function of ξ so that the optical thickness $d(\xi)$ does not reach that "threshold" value at which there is a change in the sign of the drift velocity. However, at low values of a the fall of the concentration is slight and as ξ increases the optical thickness $d(\xi)$ reaches its threshold and then the drift velocity changes its sign and the rise of the concentration begins.

[1] F. Kh. Gel'mukhanov and A. M. Shalagin, Pis'ma Zh. Eksp. Teor. Fiz. **29**, 773 (1979) [JETP Lett. **29**, 711 (1979)].
[2] F. Kh. Gel'mukhanov and A. M. Shalagin, Zh. Eksp. Teor. Fiz. **78**, 1672 (1980) [Sov. Phys. JETP **51**, 839 (1980)].
[3] A. K. Popov, A. M. Shalagin, V. M. Shalaev, and V. Z. Yakhnin, Zh. Eksp. Teor. Fiz. **80**, 2175 (1981) [Sov. Phys. JETP **53**, 1134 (1981)].
[4] S. N. Atutov, St. Lesjak, S. P. Pod'yachev, and A. M. Shalagin, Opt. Commun. **60**, 41 (1986).
[5] S. N. Atutov, I. M. Ermolaev, and A. M. Shalagin, Zh. Eksp. Teor. Fiz. **92**, 1215 (1987) [Sov. Phys. JETP **65**, 679 (1987)].
[6] V. N. Panfilov, V. P. Strunin, P. L. Chapovskiĭ, and A. M. Shalagin, Pis'ma Zh. Eksp. Teor. Fiz. **33**, 52 (1981) [JETP Lett. **33**, 48 (1981)].
[7] A. D. Streater, J. Mooibroek, and J. P. Woerdman, Opt. Commun. **64**, 137 (1987).
[8] S. N. Atutov and A. M. Shalagin, Opt. Spektrosk. **64**, 223 (1988) [Opt. Spectrosc. (USSR) **64**, 133 (1988)].
[9] S. N. Atutov and A. M. Shalagin, Pis'ma Astron. Zh. **14**, 664 (1988) [Sov. Astron. Lett. **14**, 284 (1988)].
[10] A. K. Popov, A. M. Shalagin, A. D. Streater, and J. P. Woerdman, Phys. Rev. A **40**, 867 (1989).
[11] A. D. Streater, Phys. Rev. A (in press).
[12] S. G. Rautian, G. I. Smirnov, and A. M. Shalagin, *Nonlinear Resonances in Spectra of Atoms and Molecules* [in Russian], Nauka, Novosibirsk (1979).
[13] I. I. Sobelman, *Atomic Spectra and Radiative Transitions*, Springer Verlag, Berlin (1979).
[14] B. M. Smirnov, *Asymptotic Methods in the Theory of Atomic Collisions* [in Russian], Atomizdat, Moscow (1973).
[15] W. Happer, Rev. Mod. Phys. **44**, 169 (1972).
[16] M. Abramowitz and I. S. Stegun (eds.), *Handbook of Mathematical Functions with Formulas, Graphs, and Mathematical Tables*, Dover, New York (1964).
[17] S. N. Atutov, S. P. Pod'yachev, and A. M. Shalagin, Zh. Eksp. Teor. Fiz. **91**, 416 (1986) [Sov. Phys. JETP **64**, 244 (1986)].

Translated by A. Tybulewicz